Scientific Research Publishing

Advances in Materials Physics and Chemistry, 2026, 16(5), 176-190
https://www.scirp.org/journal/ampc
ISSN Online: 2162-5328
ISSN Print: 2162-531X

Understanding the Combined Effects of Structural and Electronic Parameters in Perovskite Solar Cells

Firmin Asmane Labidi Lompo, Soumaïla Ouédraogo, Boureima Traoré, Issiaka Sankara, Valentin Tapsoba, François Zougmoré

Département de Physique, Laboratoire de Matériaux et Environnement (LA.M.E)-UFR/SEA, Université Joseph Ki-Zerbo, Ouagadougou, Burkina Faso
Email: labidilompo@gmail.com, ouedraogosoumaila@gmail.com, traoreboureim@gmail.com, sankaraissaka@gmail.com, valpero2018@gmail.com, zougfran2013@gmail.com

How to cite this paper: Lompo, F.A.L., Ouédraogo, S., Traoré, B., Sankara, I., Tapsoba, V. and Zougmoré, F. (2026) Understanding the Combined Effects of Structural and Electronic Parameters in Perovskite Solar Cells. *Advances in Materials Physics and Chemistry*, **16**, 176-190.
https://doi.org/10.4236/ampc.2026.165009

Received: April 19, 2026
Accepted: May 24, 2026
Published: May 27, 2026

Abstract

This article presents a numerical study of three-dimensional halogenated perovskite solar cells based on $CH_3NH_3PbI_{3-x}Cl_x$, a benchmark material in high-efficiency photovoltaics. Using SCAPS-1D software, the influence of physical parameters such as thickness, hole mobility, and doping level on the performance of the perovskite solar cell was investigated. The simulations, based on solving the Poisson and continuity equations, show that doping and hole mobility play a decisive role in optimizing the open-circuit voltage and fill factor, while the short-circuit current density is primarily limited by recombination. The model is validated by direct comparison with a published reference device, showing excellent agreement. The results highlight that moderate to high doping levels (10^{18} to 3×10^{18} cm^{-3}), combined with high mobility and a thickness of approximately 800 nm, optimize performance. Higher doping and the presence of a hole transport layer (HTL) are found to specifically improve V_{OC} and FF, whereas the absorber thickness strongly controls the overall efficiency. The integration of a hole transport layer enhances charge extraction, limits recombination, and enables efficiencies exceeding 20%.

Keywords

Perovskite, $CH_3NH_3PbI_{3-x}Cl_x$, Optimize Performance, SCAPS 1D, Hole Transport Layer

1. Introduction

The three-dimensional perovskite of general formula $CH_3NH_3PbI_{3-x}Cl_x$ (x = 1, Br

or Cl) has emerged as a leading material in the field of photovoltaics since its emergence in 2012. Within a few years, it has experienced rapid development, and has become one of the most efficient materials, with a certified power conversion efficiency reaching 22% according to the National Renewable Energy Laboratory (NREL) [1]. This progress is mainly attributed to its superior transport properties, characterized by high charge carrier mobility [2] [3], as well as its high absorption coefficient in the solar spectrum [4] [5]. Another key advantage lies in its remarkable chemical flexibility, which enables precise molecular engineering of its constituents and the fine-tuning of its physical and electronic properties [6]. More recently, halide perovskites have also demonstrated considerable potential as active materials in optoelectronic devices, particularly for light-emitting diodes and lasers [7] [8]. Nevertheless, despite the rapid advances observed in the development of perovskite-based devices, especially solar cells, the fundamental properties of these materials remain only partially understood and insufficiently documented. Identifying the physical mechanisms underlying these exceptional performances, as well as establishing robust correlations between optical and excitonic properties, morphology, and the atomic structure of the material, therefore constitute major scientific challenges for improving the performance and reliability of future devices [9] [10].

This article provides a systematic analysis of the impact of several physical and technological parameters on the performance of photovoltaic devices. The study focuses on the role of thickness, hole mobility, and doping level, as well as the coupled effect of hole mobility and doping within the absorber layer on the overall electrical parameters of perovskite solar cells. In contrast to prior SCAPS-1D optimization studies that have typically varied individual parameters in isolation (e.g., [11] focusing on defect density and band discontinuities, or [12] examining hybrid electron transport layers), the specific novelty of this work lies in its systematic mapping of the combined, two dimensional effects of hole mobility versus doping concentration and hole mobility versus absorber thickness regimes arising from different simulation conditions. Namely, carrier collection versus light absorption and provides a direct comparative analysis of devices with and without a hole transport layer, thereby offering a more integrated understanding of parameter interdependencies.

2. Materials and Methods

2.1. Structure and Operating Principle of the Perovskite Solar Cell

A perovskite solar cell is composed of a stack of thin films, with a typical thickness ranging from a few hundred nanometers to a few micrometers, deposited on a substrate, as schematically illustrated in **Figure 1**. Its operating principle is based on the absorption of incident light radiation by the perovskite active layer, which generates free charge carriers in the form of electron-hole pairs, which are subsequently extracted by selective contacts. The perovskite layer, located at the core of the device architecture, constitutes the main photoactive element [14]. When in-

cident sunlight in the visible range reaches this layer, electrons are excited from the valence band to the conduction band, generating holes simultaneously. The exciton binding energy in perovskite materials is on the order of a few tens of meV at room temperature [15]. The photogenerated electrons and holes are selectively transported by a hole transport layer (HTL) and an electron transport layer (ETL), positioned on either side of the perovskite layer [16]. These charge carriers diffuse towards the contact electrodes of the photovoltaic device, namely the transparent conducting electrode and the counter-electrode, where they are extracted, enabling the conversion of light energy into electrical energy [17].

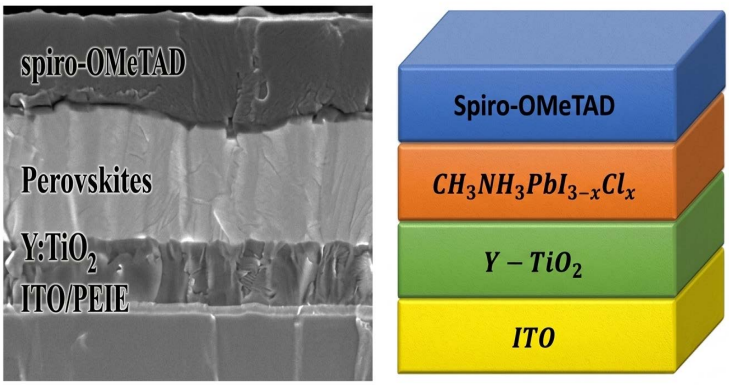

(a) (b)

Figure 1. (a) Image of a perovskite solar cell [13]; (b) Structure of a perovskite based solar cell.

2.2. Simulation Software Using SCAPS-1D

The simulation tools developed by research communities are currently available under both free and commercial licenses. Among the most widely used freely accessible simulation platforms are AFORS-HET (Automat FOR Simulation of HET erojunctions), ASA (Amorphous Semiconductor Analysis), AMPS-1D (Analysis of Microelectronic and Photonic Structures), and SCAPS-1D (Solar Cell Capacitance Simulator) [18].

SCAPS-1D is a one-dimensional numerical simulation code operating in a Windows environment, developed by the team of Marc Burgelman within the Department of Electronics and Information Systems (ELIS) at Ghent University, Belgium. Its development was initially based on modeling work dedicated to CdTe and Cu (In, Ga) Se_2 solar cells [17] [18]. SCAPS-1D is used to simulate thin-film perovskite solar cells as it solves the fundamental charge transport equations and analyzes the influence of material physical parameters on photovoltaic performance. It thus constitutes an effective tool for modeling interfaces, defects, and recombination mechanisms for optimizing the structure and efficiency of photovoltaic devices.

Numerous studies have shown that the results provided by SCAPS-1D exhibit excellent agreement with experimental data [19]-[21], as well as with those ob-

tained from the AMPS-1D software.

SCAPS-1D enables a detailed analysis of the main electrical and optoelectronic characteristics of photovoltaic devices, including J-V, C-V, and C-f characteristics, and external quantum efficiency (EQE), under both illuminated and dark conditions [22]. The model explicitly incorporates defect related mechanisms responsible for charge carrier recombination. In this context, the charge carrier recombination rate, denoted as R, is given by Equation (1) [23]:

$$R = \frac{1}{\tau_n} \frac{pn - nj_e^2}{2n_{je} + p + n}. \tag{1}$$

Given that n is the free carrier density, p is the hole concentration, n_{je} is the intrinsic carrier density, and τ_n is the electron lifetime, the generation of charge carriers resulting from the optical excitation of the material is described quantitatively by Equation (2) [23]:

$$G(z) = -\frac{\mathrm{d}\Phi}{\mathrm{d}z} = \alpha_x \Phi(z_0) \exp\left(-\alpha_x (z - z_0)\right). \tag{2}$$

where Φ is the photon flux density per unit area and time, α_x is the absorption coefficient, $\Phi(z_0)$ is the flux density at an initial depth z_0, and z represents the penetration depth of the flux.

For reproducibility, the following additional SCAPS-1D parameters were used; front contact work function (ITO) = 4.7 eV, back contact work function (Au) = 5.1 eV (typical for high work function metals); interface defect density at both ETL/perovskite and perovskite/HTL interfaces 1×10^{10} cm^{-2} (neutral, single energy level at mid gap, capture cross sections 1×10^{-19} cm^{-2} for electrons and holes, based on common practice in perovskite SCAPS modeling) [24]; absorber bulk defect model (single neutral acceptor) like defect at mi gap with total density N_t = 1×10^{13} cm^{-3} as given in **Table 1** (capture cross sections 1×10^{15} cm^{-2} for both carriers); temperature = 300 K (standard room temperature). The absorption coefficient of $CH_3NH_3PbI_{3-x}Cl_x$ was modeled using the built-in optical model of SCAPS-1D with a constant absorption coefficient of 1×10^5 cm^{-1} above bandgap, consistent with literature values for this material.

2.3. Device Characterization

SCAPS-1D simulation software (version 3.2.0.9) was employed for the numerical modeling of the device. The considered perovskite solar cell architecture adopts the following multilayer configuration: TCO/ETL/Perovskite/HTL. The conclusions drawn from this study are specifically valid for the architecture ITO/Y-TiO_2/$CH_3NH_3PbI_{3-x}Cl_x$/Spiro-OMeTAD and may not be directly transferable to other perovskite compositions (e.g., mixed cations or lead-free perovskites) or alternative charge transport layers (e.g., inorganic HTLs like NiO_x or different ETLs like SnO_2). **Table 1** summarises all the input parameters associated with the different layers of the cell, namely the transparent conductive oxide layer, the electron transport layer, the absorber layer, and the hole transport layer, composed of ITO, Y-TiO_2, $CH_3PbI_{3-x}Cl_x$, and Spiro-OMeTAD, respectively.

Table 1. Electrical parameters [13] [21] [25]-[27].

Material	Spiro-OMeTAD	$CH_3NH_3PbI_{3-x}Cl_x$	Y-TiO_2	ITO
W (nm)	100	variable	30	80
E_g (eV)	3.0	1.55	3.2	3.6
χ (eV)	2.45	3.9	4.0	4.5
ε_r (F·cm^{-1})	3.0	18	9	9.0
N_C (cm^{-3})	2.2×10^{18}	2.2×10^{18}	2×10^{18}	2.2×10^{18}
N_v (cm^{-3})	1.9×10^{19}	1.8×10^{18}	1.8×10^{19}	1.8×10^{19}
$V_{th,n}$ (cm/s)	1.0×10^{7}	1.0×10^{7}	1.0×10^{7}	1.0×10^{7}
$V_{th,P}$ (cm/s)	1.0×10^{7}	1.0×10^{7}	1.0×10^{7}	1.0×10^{7}
μ_n (cm^2/Vs)	2.0×10^{-4}	2.7	20	10
μ_P (cm^2/Vs)	2.0×10^{-4}	variable	10	10
N_D (cm^{-3})	0	0	9.6×10^{17}	1.0×10^{21}
N_A (cm^{-3})	1.7×10^{17}	variable	0	0
N_t (cm^{-3})	1.0×10^{15}	1.0×10^{13}	1.0×10^{15}	1.0×10^{14}

SCAPS-1D is employed for the modeling and analysis of thin-film solar cells, primarily developed for research applications, incorporating various buffer layer architectures. The simulation environment provided by SCAPS-1D provides access to detailed results, including current-voltage characteristics under both dark and illuminated conditions, as well as their evolution as a function of temperature. Furthermore, the software facilitates the extraction of the internal electric field, spatial profiles of free and trapped carrier concentrations, recombination mechanisms, and the associated electron and hole current densities as a function of position within the device [22]. The determination of the electrical parameters of the cell using SCAPS-1D is based on the coupled numerical solution of three fundamental equations governing charge transport in semiconductors: Poisson's Equation (3) and the continuity Equations for electrons (4) and holes (5) [28].

$$\frac{\mathrm{d}}{\mathrm{d}x}\left[-\varepsilon(x)\frac{\mathrm{d}\psi(x)}{\mathrm{d}x}\right]=\frac{e}{\varepsilon_0\varepsilon_r}\left[p(x)-n(x)+N_D^+(x)-N_A^-(x)+\rho_p-\rho_n\right] \tag{3}$$

$$\frac{\mathrm{d}}{\mathrm{d}x}J_n(x)-e\frac{\partial_n(x)}{\partial t}-e\frac{\partial\rho_n}{\partial t}=G_n(x)-R_n(x) \tag{4}$$

$$\frac{\mathrm{d}}{\mathrm{d}x}J_p(x)-e\frac{\partial_p(x)}{\partial t}-e\frac{\partial\rho_p}{\partial t}=G_p(x)-R_p(x) \tag{5}$$

where ε_0 and ε_r are the dielectric constants of vacuum and the relative dielectric constant, respectively; n and p are the free carrier concentrations (electrons and holes), respectively; N_D^+ and N_A^- denote the ionized donor and acceptor concentrations, respectively; ρ_p and ρ_n represent the charge densities of holes and electrons, respectively; J_n and J_p are the electron and hole current densities, respectively; R_n and R_p are the electron and hole recombina-

tion rates, respectively; and G_n and G_p are the electron and hole generation rates, respectively

2.4. Model Validation

The validation of our model using SCAPS-1D is based on several essential aspects to ensure that the simulation accurately reflects physical and experimental reality. The J-V curves under AM1.5G illumination enable the evaluation of the electrical performance of a solar cell by measuring several key parameters. The short-circuit current density (J_{SC}) represents the maximum current generated at zero voltage, while the open-circuit voltage (V_{OC}) corresponds to the maximum voltage under no current flow. The fill factor (FF) quantifies the quality of the J-V curve, and the power conversion efficiency (PCE) indicates the overall performance of the cell. Furthermore, all simulations are performed under AM 1.5 illumination, with an incident power of 1000 W/m^2. **Table 2** presents the values of the electrical parameters. The baseline device (without intentional variations of thickness, doping, or mobility) was reproduced directly using the material parameters reported by [13] as listed in **Table 1**, without any additional calibration or fitting. The excellent agreement between our simulated J-V curve and the experimental reference from [13] (**Figure 2**) confirms that the input parameter set accurately captures the reference device behavior.

Table 2. Values of the electrical parameters.

Type	V_{OC} (V)	J_{SC} (mA/cm^2)	FF (%)	PCE (%)
[13]	1.13	22.75	75.01	19.3
Our study	1.08	22.75	77.81	19.30
Absolute difference ($V_{exp} - V_{sim}$)	0.05	0	−2.8	0
Relative difference $\frac{V_{exp} - V_{sim}}{V_{exp}} \times 100\%$	4.42	0	−3.73	0

The electrical parameters of our model show excellent agreement with those reported by Zhou and colleagues (**Table 2**) [13]. Furthermore, the current density-voltage characteristics curves are in good accordance (**Figure 2**).

3. Results and Discussion

In the following subsections, the varied parameter is clearly identified for each study: Section 3.1 varies the hole mobility (μ_p) and the acceptor doping concentration (N_A) of the absorber layer ($CH_3NH_3PbI_{3-x}Cl_x$); Section 3.2 varies the hole mobility (μ_p) and the thickness (W) of the absorber layer; Section 3.3 varies the acceptor doping concentration (N_A) of the absorber layer; Section 3.4 varies the thickness (W) of the absorber layer. The hole transport layer (HTL) doping remains fixed at the value given in **Table 1** unless otherwise stated.

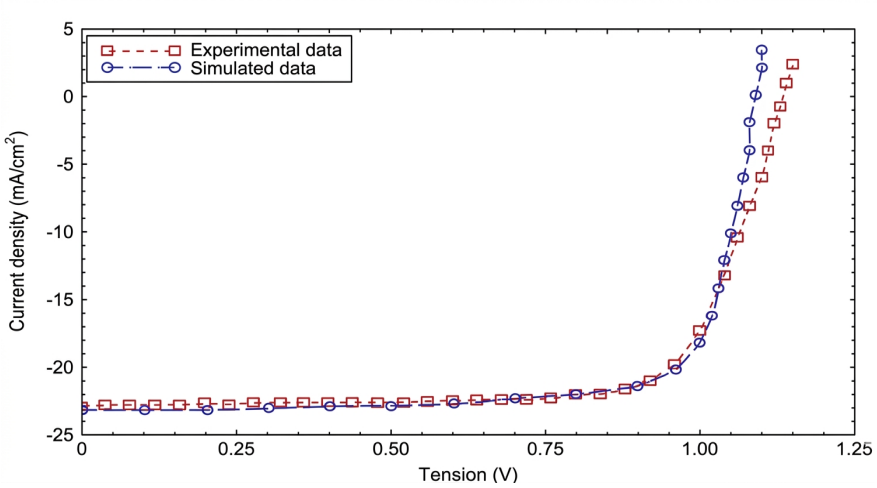

Figure 2. Modeling results obtained with the parameters from **Table 1**, compared with the experimental results from [13].

3.1. Hole Mobility as a Function of Absorber Layer Doping

The hole mobility of the absorber layer in a perovskite solar cell governs the transport and collection efficiency of photogenerated charge carriers, thereby directly influencing the current density, fill factor, and overall device performance. Investigating its variation as function of doping enables the identification of the optimal doping level that enhances charge separation and the internal electric field while limiting recombination and carrier diffusion. The coupling between hole mobility (μ_p) and the acceptor doping concentration (N_A) of the absorber layer governs the stable operating regime of the solar cell. Low doping level result in an insufficient internal field, making the device performance highly sensitive to transport limitations and recombinations [12]. Conversely, high doping reduces the influence of μ_p but accentuates intrinsic recombinations, thereby capping performance. An intermediate doping level ensures an optimal trade-off between carrier transport and the internal electric field, characterized by a low sensitivity of the electrical parameters. We varied the hole mobility between 2×10^{-4} cm²/V·s and 10^{-2} cm²/V·s, and the doping concentration between 3×10^{17} cm^{-3} and 3×10^{18} cm^{-3}. **Figure 3** highlights the combined influence of the absorber layer doping and hole mobility on the electrical performance and overall electrical stability of the device. Overall, the device performance is primarily governed by these factors. The results show that the open-circuit voltage (V_{OC}) is strongly influenced by doping: it increases almost continuously from 0.90 V to 1.08 V as the doping concentration rises from $3 \times 3 \times 10^{17}$ cm^{-3} to 3×10^{18} cm^{-3}. In contrast, hole mobility has a negligible effect, with variations limited to a few millivolts, underscoring the dominant role of the internal field and recombinations [12]. Conversely, the fill factor is largely governed by mobility and device architecture; it increases from 75% - 77% at low doping to 86% - 87% at high doping, reflecting a reduction in resistive losses [29]. The short-circuit current density systematically decreases with increasing doping due to enhanced recombination [30]. The efficiency,

therefore, results from a trade-off between the increase in open-circuit voltage and fill factor and the decrease in short-circuit current density, reaching a plateau of 16.4% with an optimized HTL [31]. Optimal stability is achieved for intermediate to high doping concentrations (1×10^{18} cm^{-3} to 3×10^{18} cm^{-3}) with hole mobility being the key parameter for operational robustness [12].

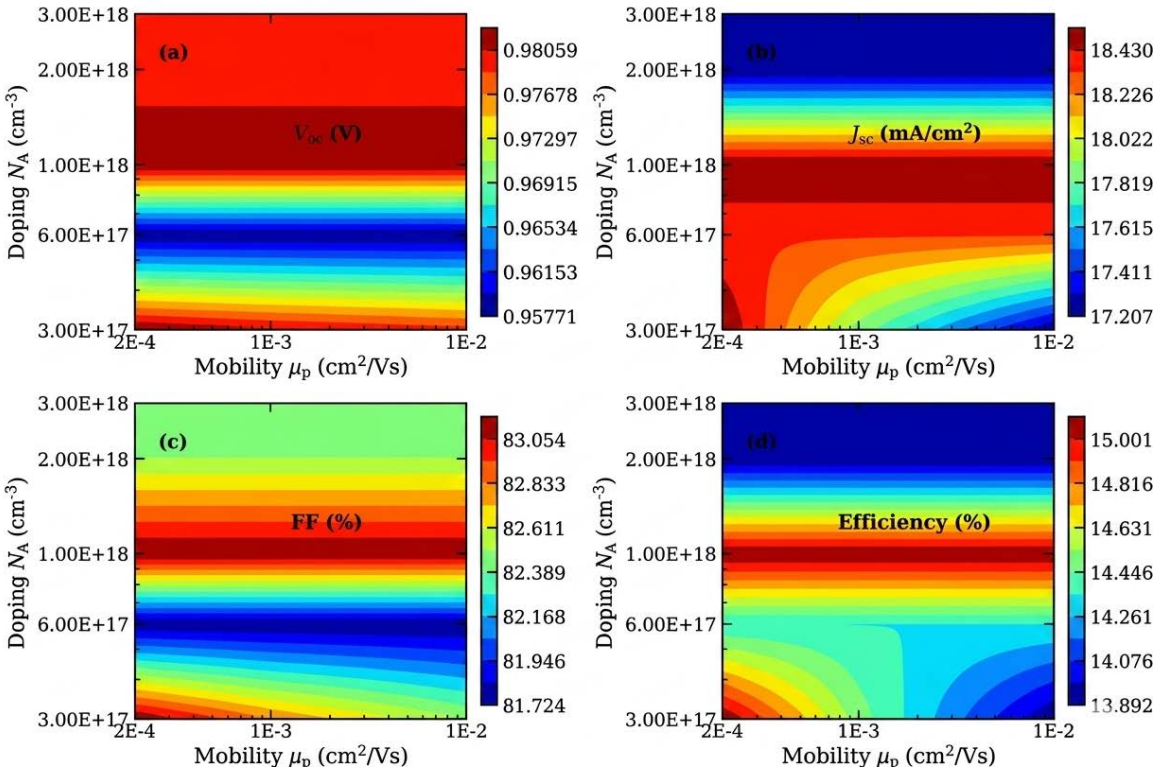

Figure 3. Influence of hole mobility as a function of absorber layer doping on cell stability.

3.2. Hole Mobility as a Function of Absorber Layer Thickness

The hole mobility (μ_p) and the thickness of the perovskite absorber layer are two critical parameters for optimizing the performance of perovskite solar cells. Hole mobility determines the efficiency of photogenerated charge transport and extraction, while the thickness of the absorber layer directly controls light absorption and carrier generation. **Figure 4** illustrates the combined influence of hole mobility (μ_p) and active layer thickness on the electrical parameters of the perovskite solar cell (PSC). Overall, it is observed that all electrical parameters of the perovskite solar cell (PSC) depend strongly on thickness, but very little on hole mobility (μ_p) within the studied range. The results show that performance is primarily governedby thickness, whereas (μ_p) exerts a negligible influence over the investigated range of 10^{-3} cm^2/V·s to 10^{-2} cm^2/V·s 1. The open-circuit voltage (V_{OC}) increases slightly with thickness due to improved absorption and a relative reduction in recombinations (**Figure 4(a)**). The short-circuit current density (J_{SC}) (**Figure 4(b)**) and the fill factor (FF) (**Figure 4(c)**) reach their maximum values for an optimal thickness between 0.06 and 0.07 μm, reflecting a trade-off between

photon absorption and bulk recombination within the absorber. Concerning the power conversion efficiency (η) (Figure 4(d)), it exhibits a maximum of approximately 15% within this same thickness range. Based on our analysis in this section, we can conclude that the performance of the perovskite solar cell (PSC) is primarily controlled by the absorber thickness, and hole mobility (μ_p) has very little influence on the performance of the perovskite solar cell (PSC) over the studied interval. Optimal performance is achieved for a thickness of approximately 0.06 to 0.07 μm. Beyond this value, recombination phenomena limit performance. These results indicate that optimization of the active layer constitutes the key determining parameter for improving the overall device efficiency.

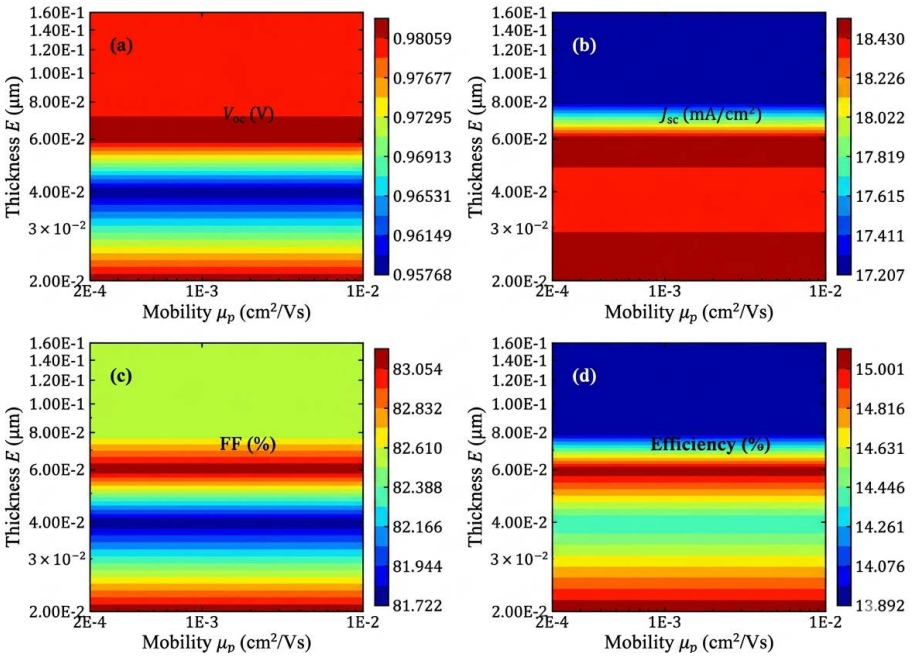

Figure 4. Influence of hole mobility as a function of absorber layer thickness on cell stability.

3.3. Influence of Absorber Layer Doping Variation on Electrical Parameters

Figure 5 illustrates the impact of absorber doping concentration ($CH_3PbI_{3-x}Cl_x$) on the performance of perovskite solar cells with and without a hole transport layer (HTL). Overall, a decrease in the performance of the perovskite solar cell is observed in the absence of the hole transport layer. The electrical parameters of both device configurations exhibit a similar trend. Increasing the doping concentration generally enhances the overall efficiency through an increase in open-circuit voltage and fill factor, despite a gradual decrease in short-circuit current density due to enhanced recombination [27] [28]. The efficiency increases at low to moderate doping levels and then stabilizes, with devices incorporating an HTL maintaining superior performance owing to more selective charge extraction [30] [31]. The open-circuit voltage increases and subsequently saturates, dominated by recombination processes within the absorber layer [31], while the short-circuit

current density decreases as a result of Shockley-Read-Hall (SRH) recombination. The fill factor improves with increasing doping concentration, with the HTL ensuring a selective back contact and superior overall device performance.

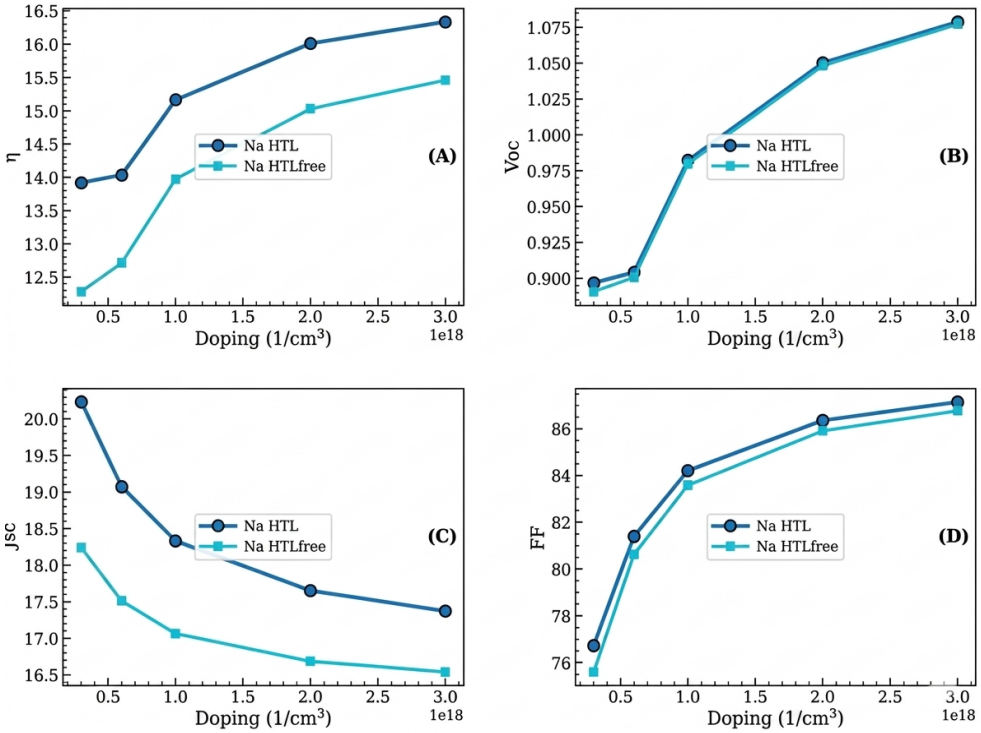

Figure 5. Influence of doping variation on electrical parameters.

3.4. Influence of Absorber Layer Thickness Variation on Electrical Parameters

In this section, we analyze the performance of the perovskite solar cell with and without the hole transport layer while varying the absorber thickness from 100 nm to 2000 nm. The comparison between architectures with and without a hole transport layer (HTL) highlights the central role of the absorber in determining photovoltaic performance. The efficiency (**Figure 6(a)**) increases rapidly with absorber thickness in both cases, but only the architecture incorporating an HTL reaches a plateau near 22%, whereas the perovskite solar cell without a hole transport layer remains limited to 8% - 9%. This underscores the importance of selective hole extraction and the reduction of interfacial recombination [32]-[34]. The open-circuit voltage (**Figure 6(b)**) is significantly penalized in the absence of an HTL (0.52 V at 1600 nm), while it stabilizes around 1.12 V with an HTL, a consequence of improved band alignment and suppression of interface defects [35]. The short-circuit current density (**Figure 6(c)**) reaches 25 mA·cm^{-2} with the hole transport layer compared to 23 - 24 mA·cm^{-2} without the hole transport layer, reflecting more efficient charge collection [36]. Finally, the fill factor (**Figure 6(d)**) remains substantially higher with an HTL due to reduced resistive losses and more

ideal diode behavior [35]-[38]. The optimal thickness (approximately 800 nm) is fully exploited only in the architecture incorporating an HTL, in agreement with recent high-efficiency devices [39]-[41].

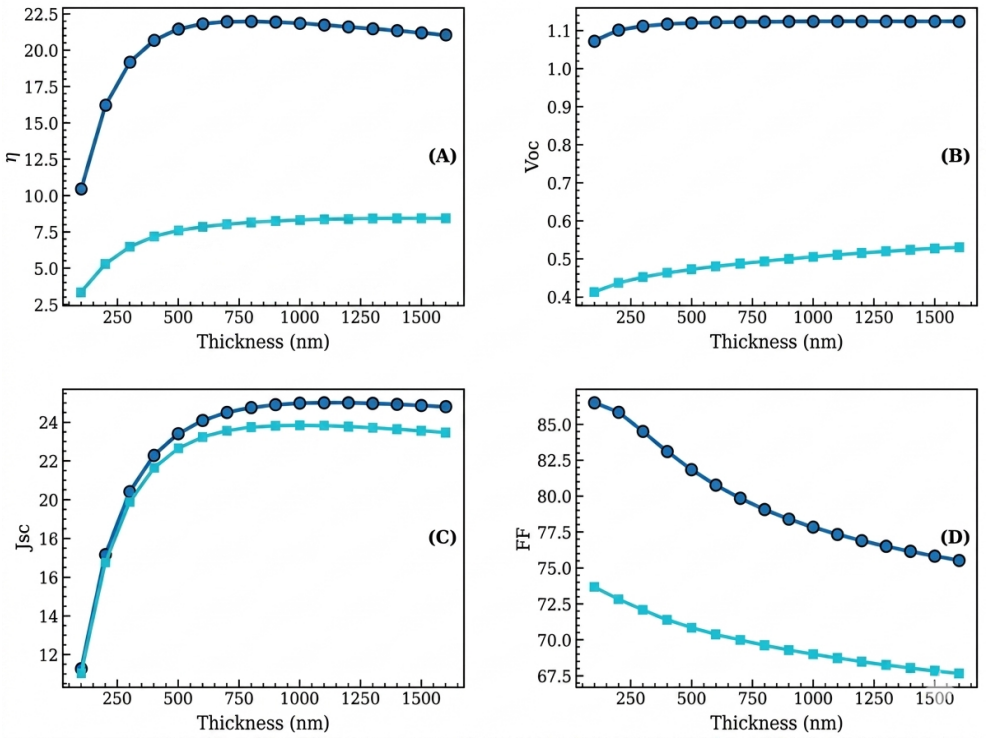

Figure 6. Influence of thickness variation on electrical parameters.

4. Conclusion

In this manuscript, we have conducted a study on the influence of hole mobility as a function of absorber layer thickness and doping concentration, as well as the combined impact of doping and thickness on the electrical parameters of a perovskite solar cell (PSC). The results highlight that the performance and stability of the device are governed by achieving an optimal trade-off between dopant concentration, carrier mobility, and absorber layer thickness. The analysis of hole mobility as a function of thickness shows that PSC performance is primarily controlled by the absorber thickness, while hole mobility exerts a negligible influence within the investigated range. Depending on the simulation range, two distinct optimal thicknesses are identified: approximately 100 - 1000 nm when scanning the very thin regime (100 - 1000 nm, where carrier collection dominates), and approximately 800 nm when scanning the conventional regime (100 - 2000 nm, where light absorption and bulk recombination dominate). The comparative study of devices with and without a hole transport layer (HTL) confirms the decisive role of this layer in improving charge carrier extraction, reducing recombination at the Perovskite/HTL interface, and enhancing overall efficiency, leading to higher and more stable performance. The identification of economical and eco-friendly alter-

natives to conventional HTLs could significantly reduce production costs while maintaining, or even improving, device performance and durability, thereby facilitating their large-scale industrialization.

Conflicts of Interest

The authors declare that they have no conflicts of interest regarding the publication.

References

[1] (2019) Chiffres clés des énergies renouvelables. https://www.statistiques.developpement-durable.gouv.fr/chiffres-cles-des-energies-renouvelables-edition-2019

[2] Ilyas, M., Kaur, K., Sharma, J. and Saini, G. (2022) DFT Study of Electronic Structure and Mobility of Pristine and Fluorinated Methylammonium Lead Halide Perovskites (CH_3 NH_3 PbX_3, X = I, Br, Cl). *International Journal of Energy Research*, **46**, 6889-6900.

[3] Xiao, C., Liu, S., Liu, X., Li, Y. and Zhang, P. (2023) Optoelectronic Evolution in Halogen-Doped Organic-Inorganic Halide Perovskites: A First-Principles Analysis. *Molecules*, **28**, Article 7341. https://doi.org/10.3390/molecules28217341

[4] Rugut, E.K., Maluta, N.E., Maphanga, R.R., Mapasha, R.E. and Kirui, J.K. (2024) Structural, Mechanical, and Optoelectronic Properties of $CH_3NH_3PbI_3$ as a Photoactive Layer in Perovskite Solar Cell. *Photonics*, **11**, Article 372. https://doi.org/10.3390/photonics11040372

[5] Moulaoui, L., Bajjou, O., Najim, A. and Rahmani, K. (2022) The Study of Electronic and Optical Properties of Perovskites $Ch_3nh_3pbcl_3$ and $CH_3NH_3PbBr_3$ Using First-Principle. *E3S Web of Conferences*, **336**, Article 00015. https://doi.org/10.1051/e3sconf/202233600015

[6] Nishat, M., Hossain, M.K., Hossain, M.R., Khanom, S., Ahmed, F. and Hossain, M.A. (2022) Role of Metal and Anions in Organo-Metal Halide Perovskites $CH_3NH_3MX_3$ (M: Cu, Zn, Ga, Ge, Sn, Pb; X: Cl, Br, I) on Structural and Optoelectronic Properties for Photovoltaic Applications. *RSC Advances*, **12**, 13281-13294. https://doi.org/10.1039/d1ra08561a

[7] Xing, J., Yan, F., Zhao, Y., Chen, S., Yu, H., Zhang, Q., *et al.* (2016) High-Efficiency Light-Emitting Diodes of Organometal Halide Perovskite Amorphous Nanoparticles. *ACS Nano*, **10**, 6623-6630. https://doi.org/10.1021/acsnano.6b01540

[8] Jabeen, N., Zaidi, A., Hussain, A., Hassan, N.U., Ali, J., Ahmed, F., *et al.* (2022) Single- and Multilayered Perovskite Thin Films for Photovoltaic Applications. *Nanomaterials*, **12**, Article 3208. https://doi.org/10.3390/nano12183208

[9] López, C.A., Abia, C., Rodrigues, J.E., Serrano-Sánchez, F., Nemes, N.M., Martínez, J.L., *et al.* (2020) Enhanced Stability in $CH_3NH_3PbI_3$ Hybrid Perovskite from Mechano-Chemical Synthesis: Structural, Microstructural and Optoelectronic Characterization. *Scientific Reports*, **10**, Article No. 11228. https://doi.org/10.1038/s41598-020-68085-0

[10] Chen, Q., Zhou, H., Fang, Y., Stieg, A.Z., Song, T., Wang, H., *et al.* (2015) The Optoelectronic Role of Chlorine in $CH_3NH_3PbI_3$(Cl)-Based Perovskite Solar Cells. *Nature Communications*, **6**, Article No. 7269. https://doi.org/10.1038/ncomms8269

[11] sankara, I., ouedraogo, S., traore, B., zongo, A., kabre, A., oubda, D., *et al.* (2025) Influence of Electron Transport Layer and Hole Transport Layer on the Performance

of Perovskite-Based Solar Cells (PSCs). *International Journal of Physics*, **13**, 16-20. https://doi.org/10.12691/ijp-13-1-3

[12] Traore, B., Tapsoba, V., Zongo, A., Ouedraogo, S., Sankara, I. and Zougmore, F. (2026) Numerical Investigation of Performance in $MAPI_{1-x}CL_x$ Perovskite Solar Cells Employing Hybrid Electron Transport Layers. *Advances in Materials Physics and Chemistry*, **16**, 69-85. https://doi.org/10.4236/ampc.2026.162004

[13] Zhou, H., Chen, Q., Li, G., Luo, S., Song, T., Duan, H., *et al.* (2014) Interface Engineering of Highly Efficient Perovskite Solar Cells. *Science*, **345**, 542-546. https://doi.org/10.1126/science.1254050

[14] Yu, H. (2024) Perovskite Solar Cells: Structure, Working Principle, and Modification Strategy. *Highlights in Science, Engineering and Technology*, **121**, 598-601. https://doi.org/10.54097/wmnz5c61

[15] Bello, S., Urwick, A., Bastianini, F., Nedoma, A.J. and Dunbar, A. (2022) An Introduction to Perovskites for Solar Cells and Their Characterisation. *Energy Reports*, **8**, 89-106. https://doi.org/10.1016/j.egyr.2022.08.205

[16] Li, Y. (2024) The Principle and Research Progress of Perovskite Solar Cells. *Highlights in Science, Engineering and Technology*, **106**, 347-352. https://doi.org/10.54097/8r7hee26

[17] Yan, M., Wang, Y., Chen, C., Ding, X., Zhai, M., Xia, Z., *et al.* (2024) Small Molecular Dibenzo[b,d]Thiophene-Based Hole Transport Materials for Tin-Lead Perovskite Solar Cell. *The Journal of Physical Chemistry Letters*, **15**, 11119-11125. https://doi.org/10.1021/acs.jpclett.4c02692

[18] Diouf, D. (2010) Cellules photovoltaïques silicium à hétérojonctions et à structures in-terdigitée en face arrière. Thèse de Doctorat, Paris 11. https://theses.fr/2010PA112229

[19] Niemegeers, A., Burgelman, M., Herberholz, R., Rau, U., Hariskos, D. and Schock, H. (1998) Model for electronic transport in $Cu(In,Ga)Se_2$ Solar Cells. *Progress in Photovoltaics: Research and Applications*, **6**, 407-421. https://doi.org/10.1002/(sici)1099-159x(199811/12)6:6<407::aid-pip230>3.0.co;2-u

[20] Khelifi, S. and Belghachi, A. (2004) Le Rôle de la Couche Fenêtre dans les Performances d'une Cellule Solaire GaAs. *Journal of Renewable Energies*, **7**, 13-21. https://doi.org/10.54966/jreen.v7i1.861

[21] Niemegeers, A. and Burgelman, M. (1997) Effects of the Au/CdTe Back Contact on IV and CV Characteristics of Au/CdTe/CdS/TCO Solar Cells. *Journal of Applied Physics*, **81**, 2881-2886. https://doi.org/10.1063/1.363946

[22] Burgelman, M., Nollet, P. and Degrave, S. (2000) Modelling Polycrystalline Semiconductor Solar Cells. *Thin Solid Films*, **361**, 527-532. https://doi.org/10.1016/s0040-6090(99)00825-1

[23] Oubda, D. (2018) Caractérisation d'une cellule solaire à couches minces à base de CIGS en fonction de la nature de la couche tampon. Thèse de Doctorat, Université Ouaga I Pr. Joseph Ki-Zerbo.

[24] Alghamdi, R.N.S., Shalaan, E.I. and Alzahrani, A.O.M. (2026) SCAPS-1D Simulation of Lead-Free Perovskite Solar Cells: Performance Analysis and Optimization. *RSC Advances*, **16**, 13875-13885. https://doi.org/10.1039/d5ra08437g

[25] Tiwari, P., Alotaibi, M.F., Al-Hadeethi, Y., Srivastava, V., Arkook, B., Sadanand, S., *et al.* (2022) Design and Simulation of Efficient SnS-Based Solar Cell Using Spiro-Ometad as Hole Transport Layer. *Nanomaterials*, **12**, Article 2506. https://doi.org/10.3390/nano12142506

[26] Basyoni, M.S.S., Salah, M.M., Mousa, M., Shaker, A., Zekry, A., Abouelatta, M., *et al.* (2021) On the Investigation of Interface Defects of Solar Cells: Lead-Based vs Lead-Free Perovskite. *IEEE Access*, **9**, 130221-130232. https://doi.org/10.1109/access.2021.3114383

[27] Li, S., Wu, Y., Zhang, C., Liu, Y., Sun, Q., Cui, Y., *et al.* (2020) Interface Modification of a Perovskite/Hole Transport Layer with Tetraphenyldibenzoperiflanthene for Highly Efficient and Stable Solar Cells. *ACS Applied Materials & Interfaces*, **12**, 45073-45082. https://doi.org/10.1021/acsami.0c12544

[28] Sankara, I., Ouédraogo, S., Oubda, D., Traoré, B., Kébré, M.B., Zongo, A., *et al.* (2023) Influence of Defect Density, Band Gap Discontinuity and Electron Mobility on the Performance of Perovskite Solar Cells. *Advances in Materials Physics and Chemistry*, **13**, 151-160. https://doi.org/10.4236/ampc.2023.138011

[29] Liu, M., Liu, H., Padmaperuma, S.R., Endo, M., Shimazaki, A., Wakamiya, A., *et al.* (2019) Influence of Hole Mobility on Charge Separation and Recombination Dynamics at Lead Halide Perovskite and Spiro-OMeTAD Interface. *Journal of Photopolymer Science and Technology*, **32**, 727-733. https://doi.org/10.2494/photopolymer.32.727

[30] Zhang, B., Lan, S., Tsai, C., Chiang, C. and Wu, C. (2025) Organic Salt-Doped Polymer Alloy: A New Prototype Hole Transporter for High-Photovoltaic-Performance Perovskite Solar Cells. *ACS Applied Materials & Interfaces*, **17**, 10674-10685. https://doi.org/10.1021/acsami.4c19907

[31] Trifiletti, V., Degousée, T., Manfredi, N., Fenwick, O., Colella, S. and Rizzo, A. (2019) Molecular Doping for Hole Transporting Materials in Hybrid Perovskite Solar Cells. *Metals*, **10**, Article 14. https://doi.org/10.3390/met10010014

[32] Deng, Z., Cui, S., Kou, K., Liang, D., Shi, X. and Liu, J. (2021) Dopant-Free Π-Conjugated Hole Transport Materials for Highly Stable and Efficient Perovskite Solar Cells. *Frontiers in Chemistry*, **9**, Article ID: 664504. https://doi.org/10.3389/fchem.2021.664504

[33] Yaghoobi Nia, N., Lamanna, E., Zendehdel, M., Palma, A.L., Zurlo, F., Castriotta, L.A. and Di Carlo, A. (2019) Doping Strategy for Efficient and Stable Triple Cation Hybrid Perovskite Solar Cells and Module Based on Poly(3-Hexylthiophene) Hole Transport Layer. *Small*, **15**, e1904399.

[34] Raza, E., Ahmad, Z., Asif, M., Aziz, F., Riaz, K., Mehmood, M.Q., *et al.* (2022) Numerical Modeling and Performance Optimization of Carbon-Based Hole Transport Layer Free Perovskite Solar Cells. *Optical Materials*, **125**, Article 112075. https://doi.org/10.1016/j.optmat.2022.112075

[35] Alanazi, T.I., Zein, W., Azab, K., Shaker, A., Salah, M.M. and Selim, D. (2024) Investigation of HTL-Free Perovskite Solar Cell under LED Illumination: Interplay between Energy Bandgap and Absorber Optimization. *Physica Scripta*, **99**, Article 055542. https://doi.org/10.1088/1402-4896/ad3c7c

[36] Chang, Q., Yun, Y., Cao, K., Yao, W., Huang, X., He, P., *et al.* (2024) Highly Efficient and Stable Perovskite Solar Modules Based on $FCPF_6$ Engineered Spiro-Ometad Hole Transporting Layer. *Advanced Materials*, **36**, Article 2406296. https://doi.org/10.1002/adma.202406296

[37] Rummaja, I.D., Idris, M.I., Napiah, Z.A.F.M., Zamani, Z.B., Ramlee, R.H. and Rashid, M. (2024) Performance Analysis of Zinc Cobaltite ($ZnCO_2O_4$) as a Hole Transport Layer (HTL) for Perovskite Solar Cell Using Oghmanano Software and Taguchi Method Optimization. *Journal of Physics: Conference Series*, **2696**, Article 012008. https://doi.org/10.1088/1742-6596/2696/1/012008

[38] Noman, M., Shahzaib, M., Jan, S.T., Shah, S.N. and Khan, A.D. (2023) 26.48% Efficient and Stable $FAPbi_3$ Perovskite Solar Cells Employing $SrCu_2O_2$ as Hole Transport Layer. *RSC Advances*, **13**, 1892-1905. https://doi.org/10.1039/d2ra06535e

[39] Ibrahim, H.K., Sabaawi, A.M.A. and Algwari, Q.T. (2021) Study of Defects in $CH_3NH_3PBi_3$-Based Perovskite Solar Cells. *IOP Conference Series*: *Materials Science and Engineering*, **1152**, Article 012032. https://doi.org/10.1088/1757-899x/1152/1/012032

[40] Qasim Agha, D.N. and Algwari, Q.T. (2021) The Influence of the Interface Layer between the Electron Transport Layer and Absorber on the Performance of Perovskite Solar Cells. *IOP Conference Series*: *Materials Science and Engineering*, **1152**, Article 012033. https://doi.org/10.1088/1757-899x/1152/1/012033

[41] Xiao, B., Zhang, W., Xiong, Y., Huang, Y., Huang, C., Qian, Y., *et al.* (2024) Energy Level Alignment Regulation and Carrier Management in Perovskite Solar Cells with Various Bandgaps Using Tailored Metal-Organic Frameworks. *Advanced Functional Materials*, **35**, Article 2417293. https://doi.org/10.1002/adfm.202417293